CIMM

Consortium for Innovation in Manufacturing & Materials

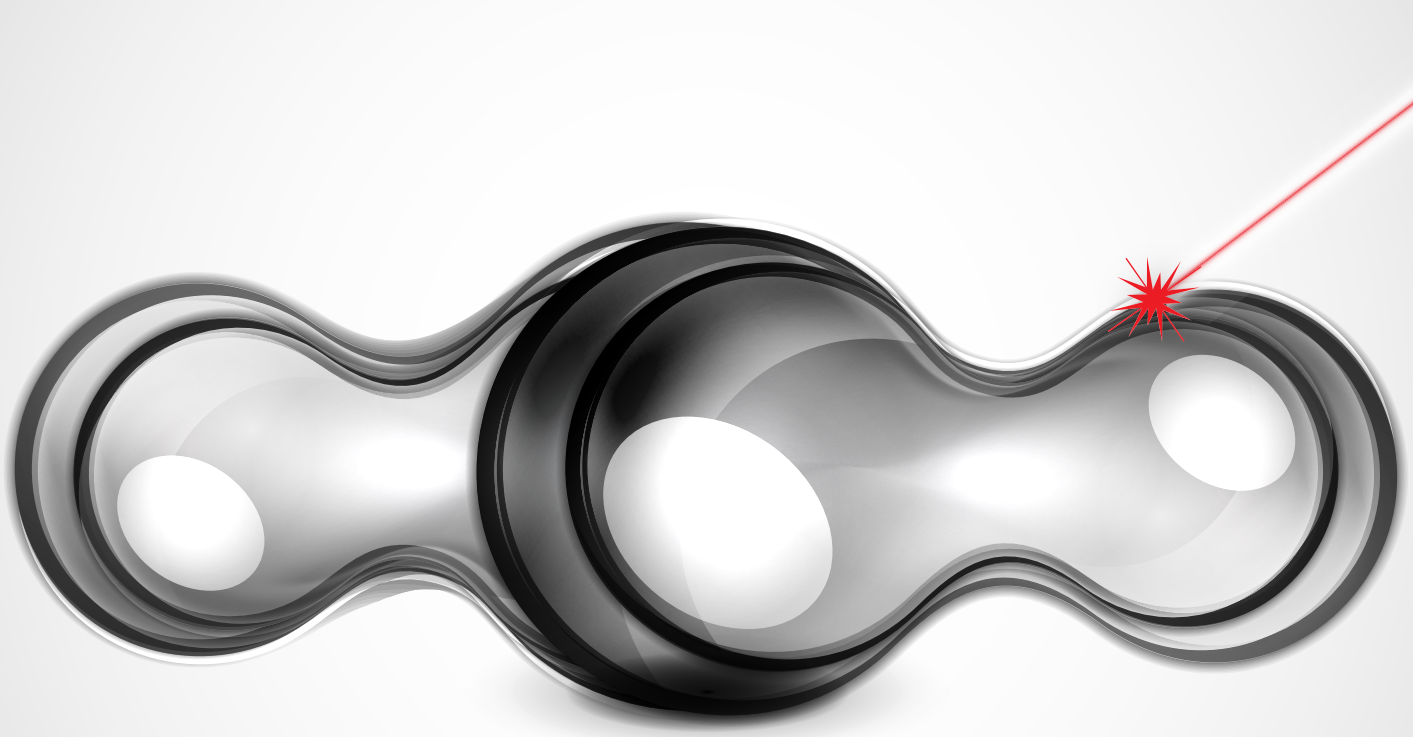

Proceedings

RII CIMM Symposium

June 3, 2019 • Baton Rouge, LA

Sponsored by the National Science Foundation, Louisiana Board of Regents and Louisiana EPSCoR.

The Design of High Temperature and Pressure Multicomponent Alloy

Congyan Zhang[1], Uttam Bhandari[1], Sai Uppu[1], Xuhang Gu[1], Gregory Richard[1], Latorious Spurlock[1], Ebrahim Khosravi[1], Patrick Mensah[2], Dwayne Jerro[2], Samuel Ibekwe[2], Guoqiang Li[3], Shengmin Guo[3], and Shizhong Yang[1]

[1]Department of Computer Science, Southern University and A&M College, Baton Rouge, LA, 70813
[2]Department of Mechanical Engineering, Southern University and A&M College, Baton Rouge, LA 70813
[3]Department of Mechanical & Industrial Engineering, Louisiana State University, Baton Rouge, LA 70803

Abstract: In this report, we designed and comparatively studied 3 refractory high entropy alloys (RHEAs) MoNbTaVW, MoNbTaTiW, and HfNbTaTiZr. The phase diagram shown that the RHEAs keep body-centered cubic when the temperature is above 1000 ℃, and the melting temperature of these alloys are above 2000 ℃. The structural and mechanical properties of the BCC RHEAs were performed by SSOS method and 100-atom super cell, the results conformed the same accuracy of both methods. The potential high strength and high ductileness of RHEAs were revealed.

Keywords: High entropy alloy, strength, ductileness, phase diagram

1. Introduction

The multicomponent alloy, which in many times also refers as high entropy alloy (HEA), generally contains five or more components with equal or near equal concentrations [1]. HEAs have been considered as the new class of advanced material because of their promising mechanical properties at high temperature. The refractory HEAs (RHEAs) are the new developed alloys in which multiple refractory elements are contained in the alloy. RHEAs were widely investigated because of the wide range in elementary properties of refractory elements, which is more flexible to design the required alloys. Some of the frequency contained refractory elements in RHEAs include Mo, Nb, Ta, Ti, V, W, Cr, Hf, Zr, and Al [2, 3]. In this report, we exhibit the structural, mechanical properties and phase diagram of several five-element RHEAs, including MoNbTaVW, MoNbTaTiW, HfNbTaTiZr, as well as pure BCC W. More possible RHEAs need to be studied to give a comprehensive understanding on the influence of typical element to the mechanical properties and phase transition of RHEAs.

2. Computational method

The density functional theory (DFT) [4, 5] framework was employed in the processes of design high strength and high ductileness HEAs. The structure optimization, and mechanical properties calculations were performed by using VASP package [6] as well as MedeA [7] software. The electron-ion interactions were described by the projector augmented wave (PAW) [8], while electron exchange-correlation interactions were described by the generalized gradient approximation (GGA) [9] in the scheme of Perdew-Burke-Ernzerhof (PBE) [10]. The structural relaxation was performed using Congregate-Gradient algorithm [11] implemented in VASP. An energy cutoff was set to be

300 eV for the plane wave basis in all calculations, and the criteria for the convergences of energy and force in relaxation processes were set to be 10^{-4} eV and 10^{-3} eV/Å, respectively. The phase diagrams were realized by using the Thermo-Calc-2019 [12] software.

3. Results and discussion

The calculated phase diagram of MoNbTaVW, MoNbTaTiW, and HfNbTaTiZr are shown in figure 1. When the temperature above 1000 ℃, the BCC is the only phase of RHEAs. On the other hand, the HCP phases appear in MoNbTaTiW and HfNbTaTiZr at low temperature, which is due to the exists of Ti. The melting temperature of MoNbTaVW is about 2700 ℃; MoNbTaTiW, 2600 ℃; and HfNbTaTiZr, 2000 ℃. The high melting temperature of RHEAs indicate their high thermal stability.

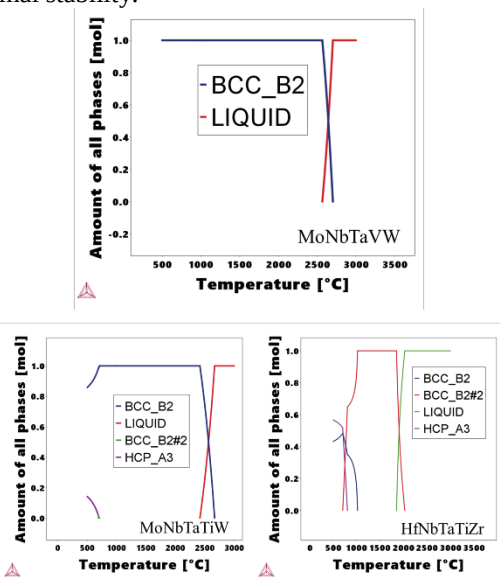

Figure 1. Phase diagram of RHEAs

Based on the phase diagram, we constructed the BCC RHEAs to explore their mechanical performance. The small set of ordered structures (SSOS) [13] were employed. As shown in figure 2, type-1 to type-3 are three different type of SSOS, the elements are distinguished by different color. The chemical component of each SSOS is $A_1B_1C_1D_1E_1$. As the comparison, we also constructed a 100-atom BCC unit cell $A_{20}B_{20}C_{20}D_{20}E_{20}$ (see type-4 in figure 2). There is no nearest pair with two same elements in the 100-atom unit cell, which indicates the high entropy of this configuration.

The structural optimization was proceeding by relaxing the RHEAs with different unit cell as shown in figure 2. The average of calculated properties from type 1 to type 3 were taken to describe the properties of RHEAs with SSOS method. The total energy per atom, equilibrium volume as well as the bulk module of RHEAs are listed in table I. For each RHEA, the total energy per atom obtained by SSOS and 100-atom unit cell are pretty close, the difference is less than 0.03 eV. In the same time, the equilibrium volume of each RHEA obtained by SSOS and

100-atom unit cell are also about the same. These illustrate that the SSOS unit cell could achieve the same accuracy as a large supercell which contains the same concentration of elements. Considering that the much smaller size of the unit cell, the SSOS method were chose to explore the mechanical properties of RHEAs.

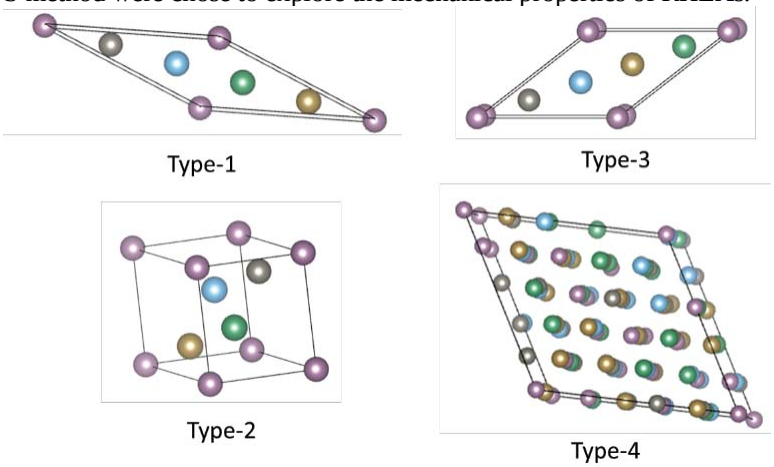

Figure 2. The BCC unit cell of HEAs, the balls in each unit cell represent the atoms; the five elements are represented by different color.

Table I. total energy per atom, equilibrium volume and bulk module of RHEAs

HEAs		**Total energy per atom (eV/atom)**	**Equilibrium volume ($Å^3$/atom)**
MoNbTaVW	SSOS	-11.026	16.05
	Type-4	-10.997	16.09
MoNbTaTiW	SSOS	-10.769	16.74
	Type-4	-10.734	16.77
HfNbTaTiZr	SSOS	-9.552	19.56
	Type-4	-9.549	19.52

The mechanical properties of RHEAs are listed in table II. The properties of pure W are also listed to compare with the alloys. As seen in table II, the bulk moduli of RHEAs are lower than that of pure W, which indicate the lower strength of RHEAs than pure W. However, the bulk moduli of these RHEAs are still much higher than other metals, for example, Cu (123GPa) [14]. The higher Pugh's ratio means higher ductile of the material. As shown in the last column of table II, the Pugh's ratio pure W at least two times smaller than that of RHEAs, which revealed the brittle of pure W and the ductile of RHEAs.

Table II. The mechanical properties of HEAs

RHEAs	Bulk module (GPa)	Shear module (GPa)	Young's module (GPa)	Poisson ratio (a.u.)	Pugh's ratio (a.u.)
W	328.26	156.27	404.61	0.2946	2.1006
MoNbTaVW	205.74	27.61	79.29	0.4358	7.4512
MoNbTaTiW	188.84	30.32	86.33	0.4238	6.2291
HfNbTaTiZr	182.92	40.36	112.79	0.3972	4.5318

4. Conclusion

In this report, we designed and comparatively studied 3 high strength and high ductile alloys MoNbTaVW, MoNbTaTiW, and HfNbTaTiZr. They keep stable BCC structure when the temperature is above 1000 ℃, and show high thermal stability. We Also compared the SSOS method and the large supercell for the theoretical prediction on RHEAs, the very close results on the properties of RHEAs obtained by both methods indicated the same accuracy. By considering the much less computer costs of SSOS method, it will be used for exploring more RHEAs with high strength and high ductile properties.

5. Acknowledgments

The current work is partially supported by the NSF EPSCoR CIMM project under award #OIA-1541079 and DoD (W911NF1910005). The Advanced Light Source is supported by the Director, Office of Science, Office of Basic Energy Sciences, of the U.S. Department of Energy (DE-AC02-05CH11231). The computation is supported by LONI computer time allocation.

6. References

[1]. J. W. Yeh, S. K. Chen, S. J. Lin, J. Y. Gan, T. S. Chin, T. T. Shun, C. H. Tsau, and S. Y. Chang, *Adv. Eng. Mater*, **6(5)** 2004, 299-303.
[2]. O. N. Senkov, G. B. Wilks, D. B. Miracle, C. P. Chuang, and P. K. Liaw, *Intermetallics*, **18** 2010, 1758-65.
[3]. O. N. Senkov, G. B. Wilks, J. M. Scott, and D. B. Miracle, *Intermetallics*, **19** 2011, 698-706
[4]. P. Hohenberg and W. Kohn, *Phys. Rev. B* **136** 1964, 864-71.
[5]. W. Kohn and L. J. Sham, *Phys. Rev. A* **140** 1965, 1133-8.
[6]. G. Kresse and J. Furthmuller, *Phys. Rev. B* **54** 1996, 11169-86.
[7]. https://www.materialsdesign.com/products
[8]. P. E. Blochl, *Phys. Rev. B* **50** 1994, 17953-79.
[9]. J. P. Perdew, J. A. Chevary, S. H. Vosko, K. A. Jackson, M.R. Pederson, D. J. Singh, and C. Fiolhais, *Phys. Rev. B* **46** 1992, 6671-87.
[10]. J. P. Perdew, K. Burke and M. Ernzerhof, *Phys. Rev. Lett.* **77** 1996, 3865-8.
[11]. H. J. Monkhorst and J. D. Pack, *Phys. Rev. B* **13** 1976, 5188-92.
[12]. J. O. Andersson, T. Helander, L. Höglund, P. F. Shi, and B. Sundman, *Calphad*, **26** 2002, 273-312.
[13]. J. Chao, and P. U. Blas, Phys. Rev. Lett. **116** 2016, 105501.
[14]. https://periodictable.com/Properties/A/BulkModulus.al.html